Basic Structures of Matter Hypothesis Based on an Alternative Concept of the Physical Vacuum

Stoyan Sarg
York University, Toronto, Ontario, Canada

Abstract: Many enigmatic phenomena in particle physics, Quantum mechanics (QM), Relativity and Cosmology can be explained in a classical 3+1 space if applying an alternative concept of the physical vacuum. This approach is adopted in the treatise titled Basic Structures of Matter (BSM), based on a space concept, closer to the Ether one but never investigated so far. The analysis of experiments and observations from a new point of view reveals that the "dark matter" is not only in distant galaxies. A model is suggested, according to which, the space may contain an underlying structure, called a Cosmic Lattice (CL), formed by two basic sub-elementary particles of two super-dens material substances, which are involved in the structure of elementary particles, as well. In a classical void space, the basic particles interact by forces inverse proportional to the cube of the distance. CL structure defines the space-time, the Quantum properties and EM fields. The complex of CL space and elementary particles defines the Newtonian gravitation, the inertia, the elementary charge and the Relativistic effects. Among the major CL properties are the Static, Partial and Dynamic pressure. The first and second one may define respectively the Newtonian mass and inertia of elementary particles. The third one is related to Zero Point Energy, which appears as two types: static and dynamic. While the second one, envisioned by Quantum mechanics, is related to EM interactions, the first one is completely hidden. It is somehow related to the nuclear energy via Newtonian mass. All known physical constants and interactions are expressible by the properties of CL space and the structure of elementary particles. CL space may propagate not only neutral Quantum waves (photons), but charge waves, as well, which are virtual particles corresponding to a Dirac "see" idea. Other major results of BSM are the unveiled atomic nuclear structures of the elements. They define the angular positions and restrictions of the chemical bonds, a feature not explainable by QM models.

*The article was presented as a poster report in the "Physics of the Third Millennium" conference, organized by NASA, Huntsville, Al, USA, 5-7 Apr 2005.

Some problems in Physics and their challenge

- **Problems of Big Bang model:** Predominating "dark matter"; accelerating Universe; supermassive black holes in balance with the galactic mass; Gamma Ray Bursts; Lyman alpha forest; redshift periodicity; small scale CMB ununiformity; experiments detecting motion of the Earth through space – **is the space of Universe void and homogenious?**
- **Could string theories be helpful in solving the problems?**

BASIC STRUCTURES OF MATTER AS A HYPOTHESIS ALTERNATIVE TO STRING THEORIES

Initial goal: Find a physical model relying on a minimum number of indestructible fundamental particles (FP) and postulates, defined in a real Euclidian space. They must build:

- an uniformly distributed spatial structure supporting all known properties of the physical vacuum;
- a hypothetical structure of the elementary particles, allowing QM and relativistic interactions between them and the physical vacuum.

Extensive analysis of phenomena from different fields of physics and natural science led to the following **adopted model**:

- **Two indestructible fundamental particles (FPs)** of two substances of intrinsic matter with a spherical shape, a radius ratio of 2:3 and different super-high density. They have a Bell shape curve dependence of the their density on the radius, which permits a spherical type of vibrations in 3D formations. They also have extremely small but different time constants, the average value of which is associated with the Planck's time: $(Gh/2\pi c^5)^{1/2} = 5.39 \times 10^{-44}$ (s) (1)
- A fundamental **law of Intrinsic Gravitation (IG),** governing the interactions between FPs in a **classical void space**, according to which FPs from a same substance are attracted by forces inverse proportional to a cube of the distance:

$$F = G_{OS} \frac{m_{01} m_{02}}{r^3} \qquad (2)$$

where: G_{OS} - intrinsic gravitational constant (between same substances), m_{01}, m_{02} intrinsic matter mass, r – distance

- **Vibrational energy:** FPs preserve a limited freedom of vibrations in formations from the same type of substance

In a complex 3D structure, FPs may vibrate within a saturation limit – an energy well of the structure. IG law could be associated with the necessary energy for filling the energy well. IG attraction between FP formations from different substances may not be strong or could become even a negative at different mutual distances due to a different time constants of both FPs.

Formations of FPs at lower level of matter organization

Tetrahedron (TH) (from FPs) Quasi Pentagon (QP) (from 5 TH)

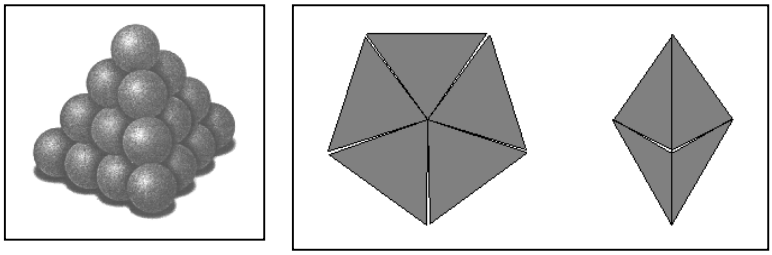

Fig. 1. Tetrahedron and Quasi Pentagon.
The rotational internal IG modes are strongest at TH and make IG fields stronger at the edges. This keeps the formations and the constant number of FPs in the formations of higher order.
1 QP = 5 PT
IG modes in QP exhibit an axial anisotropy due to its shape.

Quasi Ball (QB) from 12 QPs

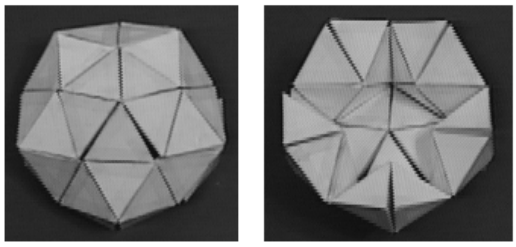

Fig. 2. Quasi Ball.
The gaps between PTs in QP are combined in a common gap of 7.355^0 which is preserved in QB. This allows left or right hand twisting of the QB - a **lowest level memory carrying the cirality.**
The sectional view of QB shows existence of internal empty space.
1 QB = 12 QP = 60 PT – equation of constant intrinsic matter quantity (preserved in upper order formations of same type)

The formational order may repeat the trend [first order QB -> second order TH –> second order QP -> second order QB…]

In Chapter 12 of BSM a scenario is presented for formation processes that may take place in a hidden phase of the evolution of every galaxy. In the center of such galaxy a large bulk intrinsic matter may exist, giving a signature of supermassive black hole. In some particular phase of galactic evolutional cycle, a matter of higher order QBs is thrown, taking a shape of concentric cloud, which collapses under IG forces. Due to the internal empty space of QBs, the highest order QBs may collapse to QPs of lower order. As a result hexagonal prisms are formed, each one containing an exact matter quantity of the highest order QB. All undestructed lower order QPs preserve the orientation of their axis due to the interactions between their anisotropic IG fields. **As a result, the prism exhibits an axial anisotropic IG field with a rotational component defined by the twisting of all embedded QBs of lower order.**

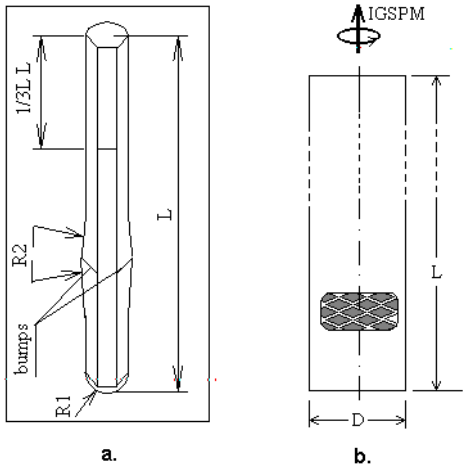

Fig. 3 Mold hexagonal prisms
a. external shape, b. internal structure from oriented QPs of same order .
IGSPM – a vector defining the axial anisotropy and handedness
Two types of prisms from a different intrinsic matter, with a linear dimension ratio 2:3 and an opposite internal twisting.

Two prisms - right and left handed, distinguishable by matter substance, size and handedness can be considered as **basic sub-elementary particles, able to build** both: the underline structure of the physical vacuum and the structures of the elementary particles.

Cosmic Lattice (CL) – structure of both types prisms, stable in empty space and uniformly distributed in the Visible Universe.

CL node – a stable formation of 4 prisms of same type hold by IG forces and possessing a flexible geometry

CL space – 3D structure of alternatively arranged CL nodes of both types prisms, like in a diamond lattice.

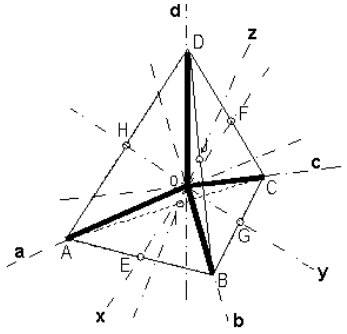

Fig. 4. CL node (4 prisms of same type)
The free ends of the prisms define a regular tetrahedron with two sets of axes of symmetry (*abcd* and *xyz*). *xyz* axes are orthogonal and coincide with the xyz axes of the neighboring four CL nodes, which are of opposite handedness.

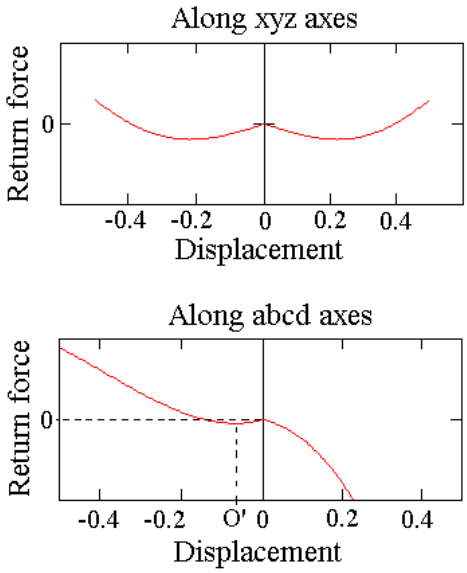

Fig 5. CL node dynamics under IG law, defined by Eq. (2)
Two minima in xyz axes and one minimum in abcd axes define a complex mode of oscillations with **two distinctive periods**. Their energy can be expressed by a precession momentum vector with origin at point 0.

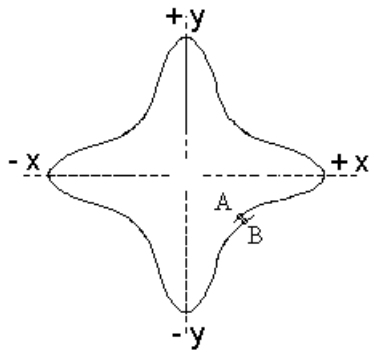

Smaller oscillation period: The node trace is almost a flat curve, however, the initial and final points do not coincide (described by a Node Resonance Momentum (NRM) vector).
Larger oscillation period: The initial and final points coincide after many NRM cycles (decribed by a Spatial Precession Momentum (SPM) Vector).
SPM forms a closed surface called SPM Quasisphere with 6 bumps (along xyz) and 4 dimples (along abcd)

Two types of SPM Quasispheres

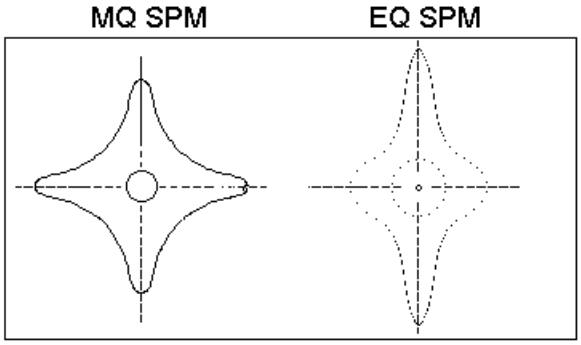

MQ (Magnetic Quasisphere) has central point symmetry.
EQ (Electrical Quasisphere) has an axial symmetry along one of ***xyz*** axes.
MQ is a normal state of CL space defining the permeability of free space.
EQ is invoked by an external charge or CL space disturbance. EQ possesses a larger energy than MQ.

Fig. 6. MQ and EQ external shape

EQ SPMs of left and right-handed CL node define the **positive** and the **negative** charge, respectively (adopted assignment). EQ can form a stationary E-filed around a particle or could be involved in a Quantum wave – a wavetrain with well defined structural arrangement and moving with a velocity of light.

Photon: A Quantum wave, containing spatially arranged positive and negative EQs. Their radial extensions are terminated by MQs, assuring boundary conditions of the photon - necessary for preservation of its energy (see Fig. 10).

Virtual particle: (from a Dirac see) a Quantum wave with only positive or negative EQs generated at specific space reaction.

Light velocity: the momentum carried by EQs is propagated between neighboring CL nodes (along *xyz*) for one NRM cycle.

In free space, (lack of EM field), MQ SPMs of the neighboring CL nodes **are spontaneously synchronized** up to a length equal to the propagation of SPM phase with a light velocity for one SPM cycle. This is a **magnetic protodomain** with a size of **Compton's wavelength.** This effect is behind the permeability of free space and assures the constancy of the velocity of light.
Magnetic line: magnetic protodomains with a size of Compton wavelength connected in loops. Consequently, the magnetic loop length is quantized - a feature apparent only in short magnetic lines, but very important for the electron's Quantum orbits in atoms and molecules.

Prisms assignment to a charge sign (valid in CL space only)
Lefthanded prism or CL node -> related to the positive charge
Righthanded prism or CL node -> related to the negative charge

Structure of elementary particles built of both types prisms.
Formations, called helical structures are result of unique crystallization process, taking place in a hidden phase of galactic evolution. The electron has only one turn of **First Order Helical Structure** (FOHS), while pions have many.

Electron: - the simplest stable formation of helical structures,

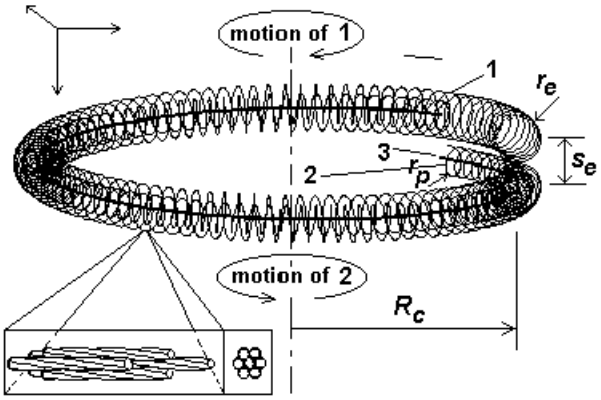

Fig. 7. Electron: contains 1 turn of 3 helical structures one inside the other (internal lattice structures are not shown)
1 – external helix of negative prisms
2 – internal helix of positive prisms
3 – internal core of negative prisms
$R_C = 3.8616 \times 10^{-13}$ (m) – Compton radius
$r_e = (3/2)r_p = 8.428 \times 10^{-13}$; $s_e = 1.77 \times 10^{-14}$ (m)

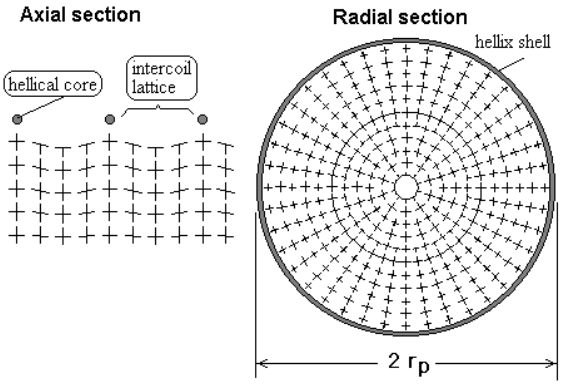

Axial and radial sections of internal Rectangular Lattice (RL) enclosed in the curved cylindrical space of the internal structure 2. Every RL node is formed of 6 positive prisms of same type. At every half distance from outer layer radius a new RL layer is formed. Prisms in radial stripes touch each other, while the tangential gap varies with layer radius.

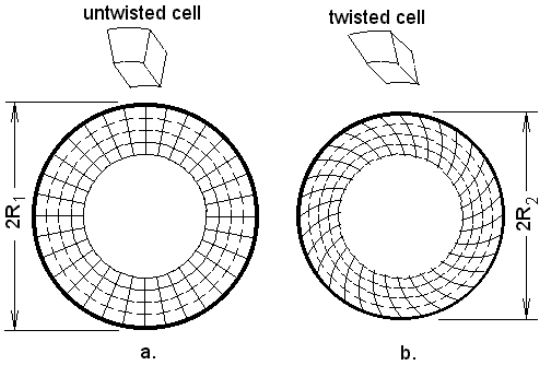

Fig. 8. The twisting of the internal RL structure stabilizes the open helical structure in CL space.
The electron's outmost RL of negative prisms with a larger whole (where the internal positive helical structure 2 is placed) is twisted.

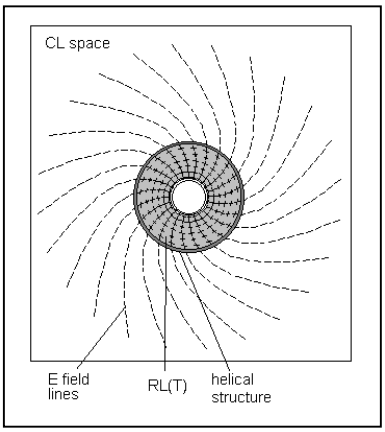

Fig. 9 The radial stripes of outmost external layer of RL structure provides a strong modulation of CL node dynamics, converting MQs to EQs. These EQs form the E-field of the helical structure – an electrical charge. In the near field E-lines are curved. This defines the rotational direction of the electron when moving in CL space. At the same time the rotating E-field causes synchronization of MQs beyond some extend, which are stabilized when connected in closed loops – magnetic lines.

Elementary charge: since E-field energy (energy of all EQs) is part of IG field energy of the twisted radial stripes, a self-supported balance of the total IG energy of the particle in CL space causes **charge constancy**. This makes the electrical charge independent from the size of the helical structure or the Newtonian mass of the particle (features - discussed in BSM).

Dynamics of the electron - a three body system with two proper frequencies:

- first proper frequency – equal to the Compton frequency (which is the SPM frequency in the Earth local field)
- second proper frequency – 3 times the Compton frequency
- the internal positive helical structure with a central negative core is an **internal positron.** Its RL(T) (of opposite handedness) cannot modulate the external CL nodes and invoke a charge, but its oscillations and phase are behind the QM spin of the electron.
- at motion, the proper frequencies could be in phase or antiphase.

The internal positron and its negative core oscillate inside the negative internal RL(T) of the electron's helical structure in conditions of ideal bearing (a symmetrically compensated IG field).

The proximity E-field of the electron causes it's **screwlike motion.** When its axial velocity is $c\alpha$, (product of light velocity and fine structure constant) the electron energy is 13.6 eV and its tangential velocity is equal to *c*. In this case, the phase of the first proper frequency matches the phase of propagated with a light velocity SPM, so this is called an **optimal confine motion** (or velocity). The rotating electron modulates the CL space up to a radius matching the known QM radius of electron.

Electron Confined motion (optimal and sub-optimal phase match)

13.6 eV – 1 turn (first harmonics – optimal confined motion)
3.4 eV – ½ turn (2nd sub-harmonic confined motion)
1.51 eV – 1/3 (3rd sub-harmonic confined motion)
0.85 eV –1/4 (4th sub-harmonic confined motion

Consequently: the subharmonic number matches the principal Quantum number of the Bohr atomic model of hydrogen.

IG field of the rotating electron invokes modulation of CL node dynamics up to a radius until the modulation velocity reaches the speed of light, where synchronized MQs are created. This is the magnetic radius. The known QM radius and Quantum magnetic field $\Phi_0 = h/e$ are at first harmonics motion. The helical step s_e causes a small advance of the electron - a signature of the "enigmatic" **anomalous magnetic moment.**

Quantum loops and orbits: Quantum loop: a closed loop for which the phases of both proper frequencies mach the phase of propagated SPM vector. The magnetic radius and magnetic line quantization (a whole number of Compton wavelengths, λ_C) also play a role. The Quantum orbits in the atoms are formed by one or more Quantum loops, connected in series. **Consequently:** The Quantum orbits are defined only by their trace length in units of λ_C .

Table 1. Quantum motion parameters of the electron in a Quantum loop

n	E (eV)	V_{ax}	V_t	r_{mb}	l_{ql}	L_q (Å)
1	13.6	αc	c	R_c	$2\pi a_0$	1.3626
2	3.4	$\alpha c/2$	$c/2$	$2R_c$	$2\pi a_0/2$	0.6813
3	1.51	$\alpha c/3$	$c/3$	$3R_c$	$2\pi a_0/3$	0.4542
4	0.85	$\alpha c/4$	$c/4$	$4R_c$	$2\pi a_0/4$	0.3406
5	0.544	$\alpha c/5$	$c/5$	$5R_c$	$2\pi a_0/5$	0.2725

n – subharmonic number, E - electron energy, V_{ax} - axial velocity, V_t - tangential velocity of rotating electron structure, α - fine structure constant, r_{mb} - equivalent magnetic radius, c - light velocity, R_c - Compton radius, a_o - Bohr radius, l_{ql} - trace length of a Quantum loop, L_q - length size of a Hippoped curve with a parameter $a=\sqrt{3}$ (close to the shape of digit 8) as an approximate shape of a real 3D Quantum orbit.

Superoptimal motion of the electron: for electron with energy larger than 13.6 eV, the resultant velocity (axial and tangential) could not exceed the light velocity, so the speed of rotation is decreased. At relativistic velocities the Quantum efficiency, η , is decreased according to Eq. (3) (derived in Chapter 3), so η in fact appears as an inverse relativistic gamma factor, γ . This effect is behind the relativistic mass increase.

$$\eta=(1-u^2/c^2)^{1/2} \text{ - Quantum efficiency} \qquad \eta=1/\gamma \qquad (3)$$

Photons generated by positronium (some of the cases): If the electron meets a free positron, both undergoes damped oscillations with Compton frequency. They pump the surrounding CL space by converting MQs to EQs. The pumped energy is released by emission of 2 photons of 511 KeV each. An undetectable neutral system of electron external shell and two inserted positrons is left. This process can be wrongly interpreted as annihilation. Oscillations with high-energy virtual positron are also possible with emission of lower energy X rays.

The electron contains an **embedded fine structure constant:**

$$s_e=\frac{\alpha\lambda_c}{(1-\alpha^2)^{1/2}} \quad \text{where: } s_e \text{ – helical step, } \lambda_c \text{ - Compton wavelength} \qquad (4)$$

Consequently, the suggested physical model of electron possesses: embedded fine structure constant; Compton radius, wavelength and frequency; features for QM spin; anomalous magnetic moment; relativistic factor; features of confined motion with preferable Quantum velocities according to equation $E=13.6/n^2$ (eV); ability for creation of magnetic field; ability to form stable Quantum loops with a Quantum mechanical lifetime [1,5]; ability to form positronium and emit X rays up to 511 KeV.

Wavetrain structure of the photon.

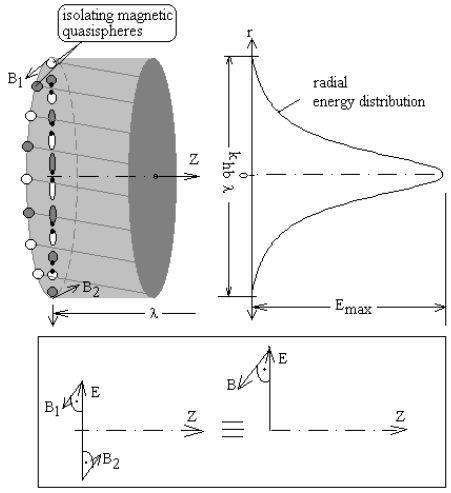

Fig. 10. Segment of photon wavetrain structure showing the arrangement of running with a light velocity EQs and MQs. EQ with a greater elongation carries a greater energy momentum. The elongation decreases with a radius, so EQs convert to MQs. This feature assures the boundary conditions of the photon that keep its energy from dissipation.

Static pressure of CL space, P_S. Since the strength of internal RL structure is about 1000 times greater than the strength of CL space, CL nodes are not able to penetrate inside of RL. Then, any helical structure with internal RL will exhibit a static CL pressure. This CL parameter is derived using the dimensions and dynamic features of the electron (BSM, Chapter 3).

$$P_S = \frac{m_e}{V_e}c^2 = \frac{g_e h v_c^{\,4}(1-\alpha^2)}{\pi\alpha^2 c^3} = 1.3735\times 10^{26} \quad (\mathrm{N/m^2}) \qquad (4)$$

where: m_e – electron mass, V_e – volume of electron's FOHS, h – Planck constant, g_e- electron's gyromagnetic ratio, v_c – Compton frequency, c – light velocity, α - fine structure constant

The similarity between the FOHS of the electron and other particles (shown below), allowed the derived Newtonian mass equation for electron to be valid for any elementary particle in a stable phase of existence (a correction factor is used for (+) FOHSs)

$$m = (P_S / c^2)V_H \quad (\mathrm{kg}) \quad \textbf{- mass equation (Newtonian mass)} \qquad (5)$$

where: P_S – CL static pressure, V_H – volume of particle FOHSs, c – light velocity

Partial pressure of CL space, P_P: Moving helical structures cause CL nodes to disconnect, partly fold, deviate, return and reconnect to their positions. In this process, they interact with the helical structure by preserving its energy momentum through CL space, defining in such way the **particle inertia**.

$$P_P = P_S \alpha \upsilon / c \quad (\mathrm{N/m^2}) \quad \text{where: } \upsilon \text{ - is velocity} \qquad (6)$$

Dynamic pressure of CL space, P_D:- related to Zero Point Waves – self synchronized MQs with a length of λ_C , responsible for the uniformity of Zero Point Energy of Dynamic type.

$$P_D = \frac{h v_c}{c S_e} = \frac{g_e h v_c^{\,3}(1-\alpha^2)}{\pi\alpha c^3} = 2.0258\times 10^3 \quad \left(\frac{N}{m^2 Hz}\right) \qquad (7)$$

The signature of P_D is the observed Cosmic Microwave Background (CMB). Consequently, **the estimated temperature of 2.72K** (by fitting of CMB to a blackbody curve) **in fact is a CL space background parameter.** The theoretical expression for this temperature is derived using a concept of ZPE waves bouncing on the proton's (neutron's) envelope (BSM Chapter 5).

$$T = \frac{N_A^{\,2}}{S_W}\frac{h v_c (R_C + r_p)^3 L_{PC}^{\,2}}{2cR_C r_e R_{ig}}\frac{\mu_e}{\mu_n} = 2.6758K \qquad (8)$$

where: S_W – reference wall area in SI (1 m^2), N_A – Avogadro number, R_{ig} – ideal gas constant, L_{PC} – length of the proton (neutron) external envelope (see Fig. 10), μ_e, μ_n - magnetic moment of electron and neutron, respectively. (μ_n is used because most emitting atoms and molecules in deep space are neutral).

The small deviation of the theoretically obtained value from experimental one could be from the physical constants, which are estimated in Earth (and solar) gravitational field, where GR effect takes place, while the CMB comes from the deep space.

Structure and shape of proton and neutron

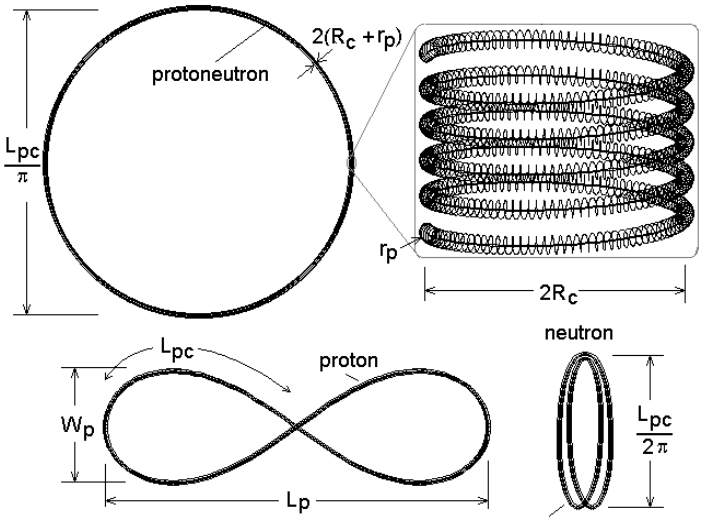

Fig. 10. Protoneutron, proton, neutron

$L_{PC} = 1.6277\dot{A} \quad L_p = 0.667\dot{A} \quad 1\dot{A} = 10^{-10}(m)$

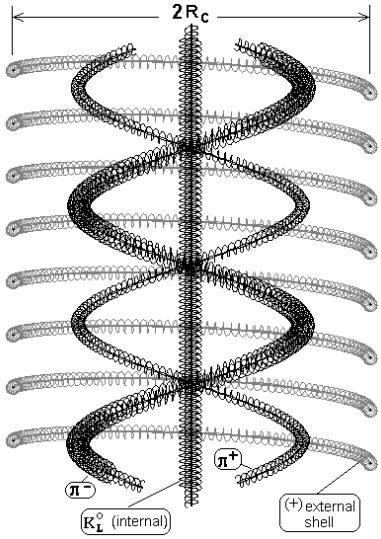

Fig. 11. Section of proton (neutron) showing internal pions and kaon

The proton (neutron) dimensions are cross validated by: (a) approximate method – from L_{PC} involvement in Eq. (8); (b) more accurately - using mass equation (5) in a mass budget balance involving accurately known energies from particle physics experiments; (c) analysis of H_2 molecule and D_2 binding energy (BSM Chapters 6,7,9)

Protons and neutrons in atomic nuclei of elements: The proton's and neutron's proximity fields define the configuration of atomic nuclei, which exhibit features matching the raw and column pattern of the Periodic table with a signature of Hunds rules and Pauli exclusion principle (in latter, the electron dynamic features also play a role). The positions of the Quantum orbits are defined by the nuclear configuration, while the energy levels are the same as the QM models. The proximity IG field and distributed E-field define a limit on the size of Quantum orbits (a problem not solved in the Bohr atomic model). In Chapter 7 of BSM, a Balmer series model is presented, giving the same energy levels. In atoms, the valence protons have a limited angular range of freedom – an important feature behind the VSEPR model in chemistry.

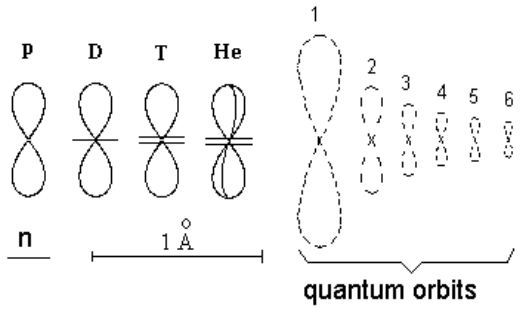

Fig. 12. Symbols used in the Atlas of Atomic Nuclear Structures (ANS):
p – proton, n – neutron, D – deuteron,
T - Tritii, He - Helium
Quantum orbits are shown by dashed line. Their size is defined by the electron confined motion sub-harmonic number, n. (see Table 1). All dimensions in scale.

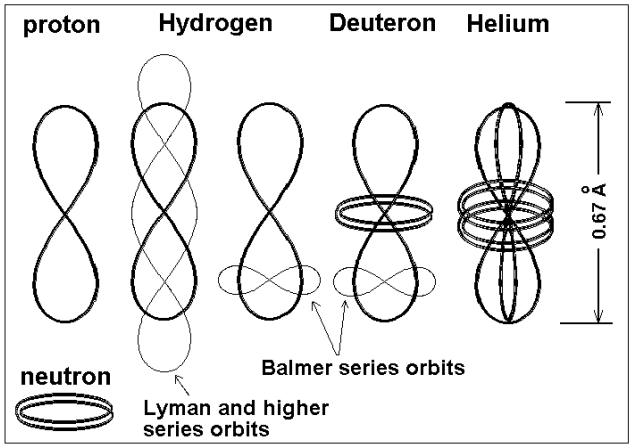

Fig. 13. Shape of simple atoms

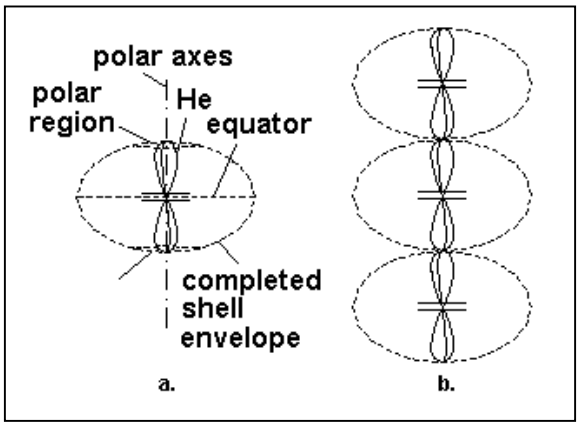

Fig. 14. a. Axial symmetry of simple atomic nucleus; b. Chain arrangement of atomic nucleus of heavier elements. Nuclear bound protons are held by a strong IG field.

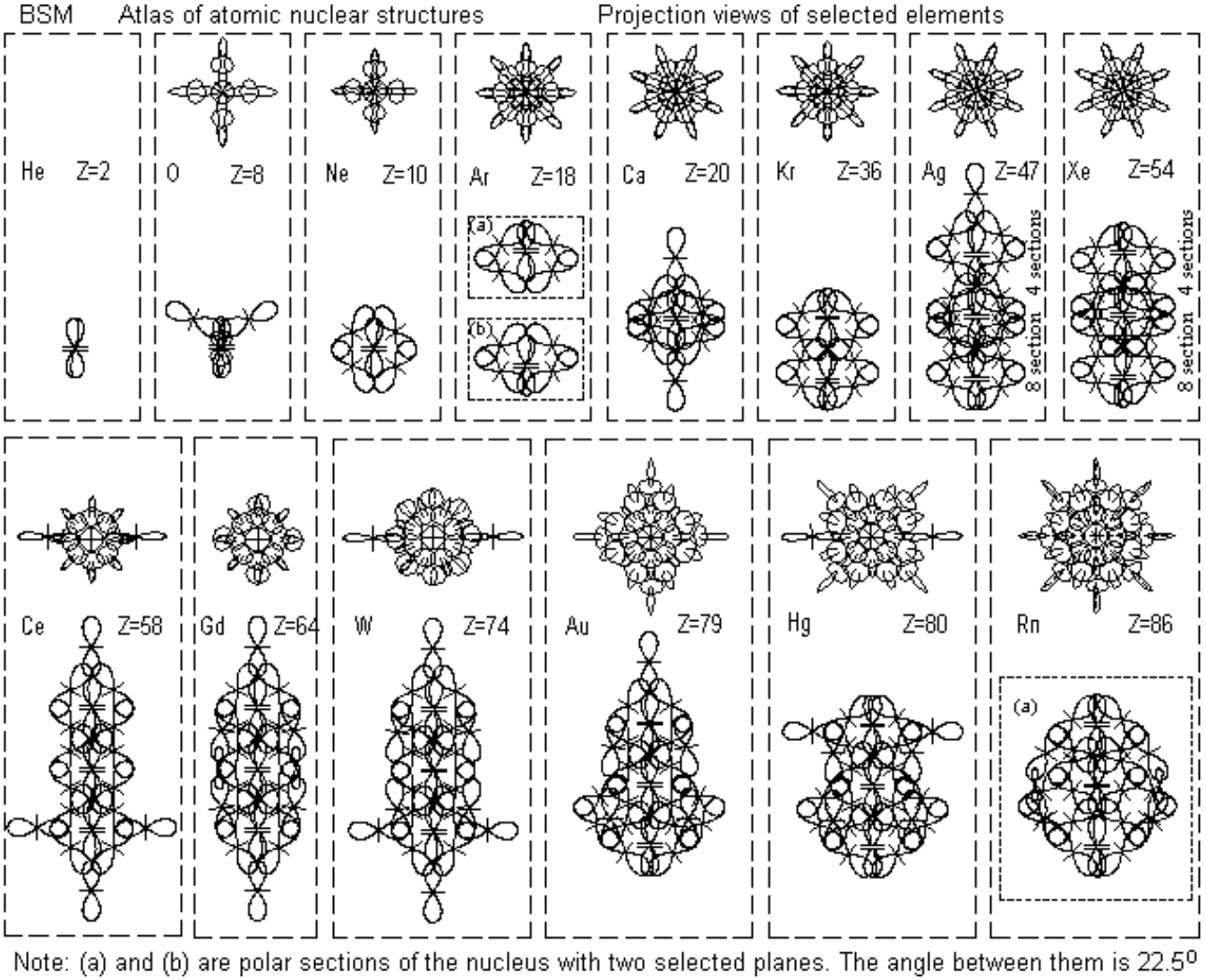

Fig. 15. Selected atomic nuclei from the ATLAS OF ATOMIC NUCLEAR STRUCTURES – one of major output results of BSM.

Atoms in molecules

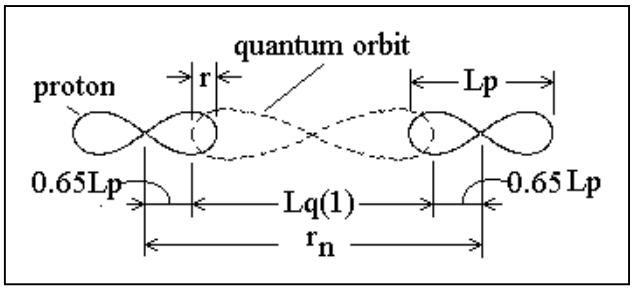

Fig. 16. H_2 – ortho-I molecule
Lp – proton length, Lq(1) – length of first harmonic quantum orbit, r_n – internuclear distance, r – position of the locus point of a Hippoped curve with parameter $\sqrt{3}$

$$E = \frac{2q}{4\pi\varepsilon_0[L_q(1) + 0.6455L_p)]} = 16.06 \text{ (eV) (BSM, Chapter 9)}$$

The total energy balance involves the energy of IG and EM fields of the system including the CL space domain. **The emission or absorption of photon is a result of a comparatively small disturbance of the total energy balance.** Eq.(9) provides example of vibrational energies of H_2:

$$E_V = \frac{C_{IG}}{q[[[(Lq(1)(1-\alpha^4\pi\Delta^2)] + 0.6455Lp]^2} - \frac{2E_q}{q} - \frac{2E_K}{q} \text{ (eV) vibrational levels} \quad (9)$$

where: $\Delta r = L_q(1)\alpha^4\pi\Delta^2$ - vibrational range; E_q – charge creation energy (511 kEv) , E_K – electron kinetic energy at optimal confine velocity , q – electron charge

$C_{IG} = G_0 m_0^2$ - IG factor (product), G_0 – IG constant, m_0 - IG mass of proton (neutron) according to IG law. The derived expression for C_{IG} is:

$$C_{IG} = (2hv_c + hv_c\alpha^2)(Lq(1) + 0.6455Lp) = 5.2651\times10^{-33}$$

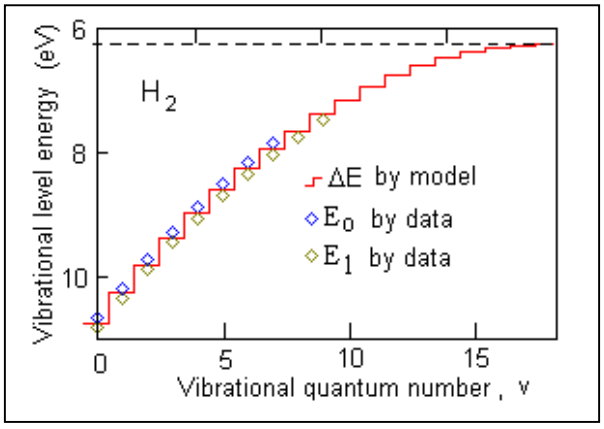

Fig. 17. Energy levels of H_2 (step line) calculated by Eq. (9) (ignoring fine structure line splitting) towards the vibrational quantum number. E_0 and E_1 data are taken from experimentally measured optical spectrum.

Important feature: Δr is extremely small, because of the strong IG field.
H_2 (and the similar D_2) system is embedded in the chemical bonds between atoms, allowing vibrational-rotational spectra). Similar equations are derived for a simple diatomic molecule. For internuclear distance of such molecule:

$$r_n = (A-p)\sqrt{\frac{2\alpha C_{IG}}{pE_B(n)}} \quad \text{internuclear distance (changes insignificantly at vibrations)} \quad (10)$$

where: A - atomic mass in Daltons (per one atom), p – number of protons involved in the bonding system, (per one atom), n – subharmonic Quantum number of the orbit, E_B – bonding energy (BSM, Chapter 9).

BSM atomic models for simple molecules (by analysis of photoelectron and optical spectra and calculating the internuclear distance using Eq. (10).

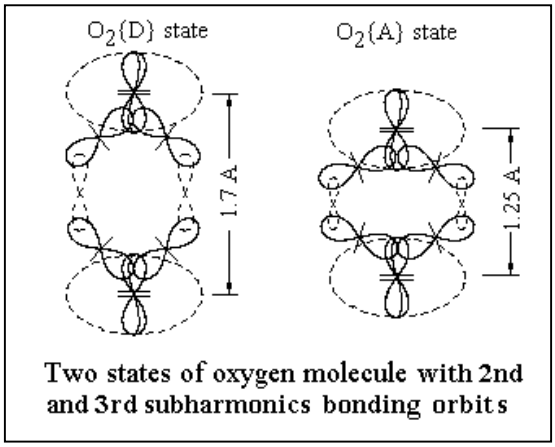

Two states of oxygen molecule with 2nd and 3rd subharmonics bonding orbits

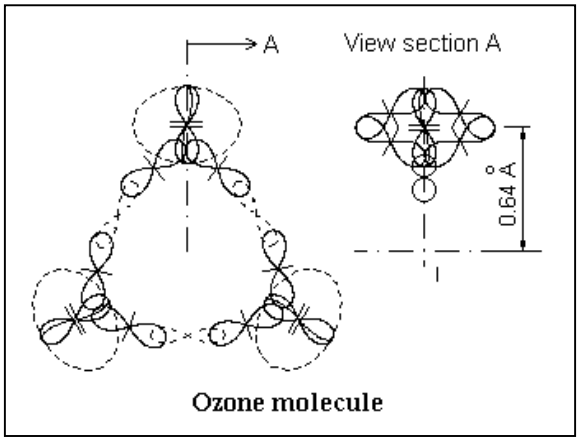

Ozone molecule

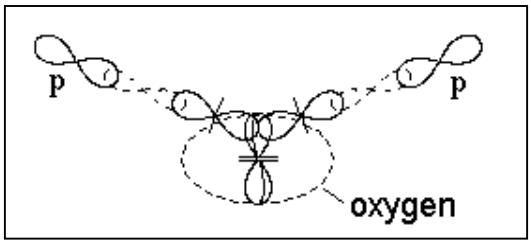

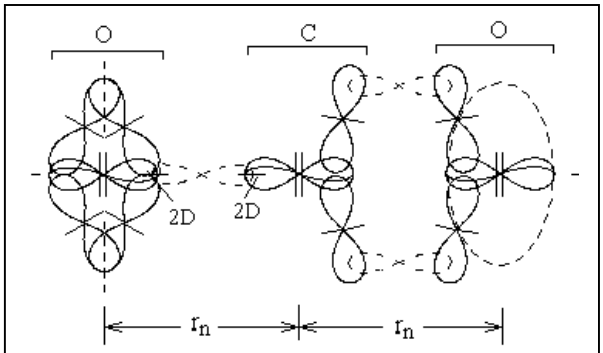

CO_2 molecule (the oxygen atoms at right and left side are rotated at 90^0)

Example of BSM atomic models for complex molecules:

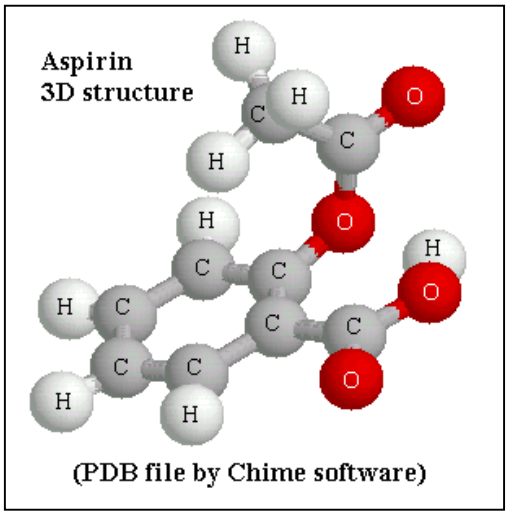

(PDB file by Chime software)

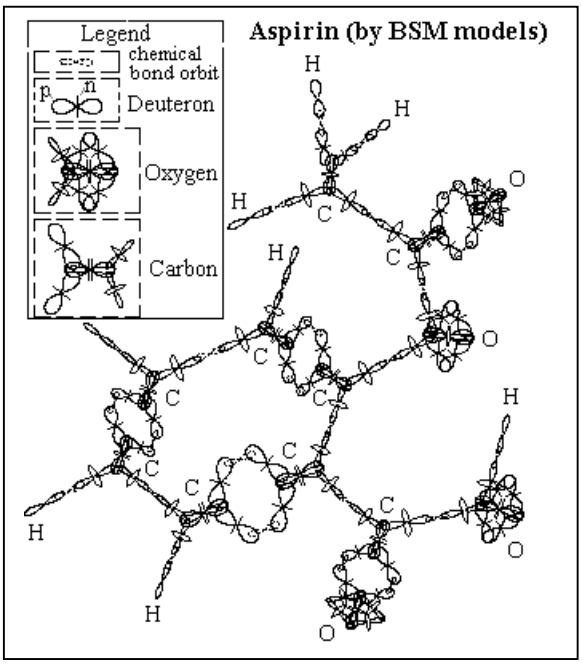

The calculated dimensions of atomic nuclei and the possible quantum orbits of BSM models match the experimentally determined internuclear distances and bond angular positions.

Atoms in metal lattice

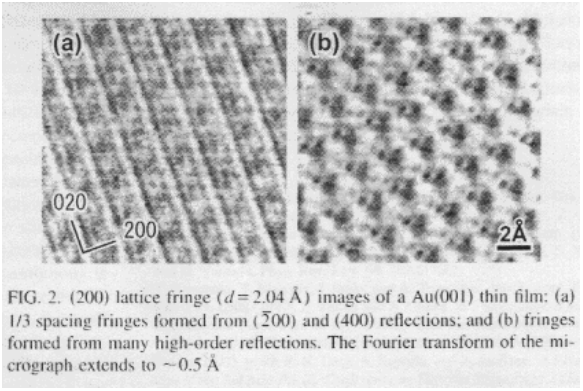

FIG. 2. (200) lattice fringe ($d = 2.04$ Å) images of a Au(001) thin film: (a) 1/3 spacing fringes formed from ($\bar{2}00$) and (400) reflections; and (b) fringes formed from many high-order reflections. The Fourier transform of the micrograph extends to ~0.5 Å

Images of two crystal planes of gold layer. Courtesy of T. Kawa-saki et al., Applied Physics Letters, v. 76, No 10, p. 1342-1344 (2000)

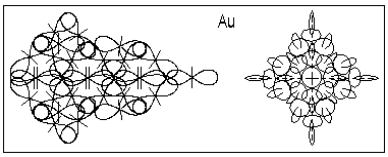

Single atom of

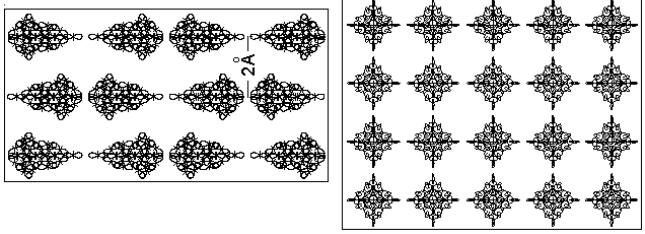

Synthetic images of a single layer of gold in two different metallic lattice planes. The internuclear distance is obtained from the BSM atomic models.

Inertia beyond Newton's first and second law (BSM, Chapter 10)

Multiplying Eq. (6) by electron structure volume we get

$$E_{IFM} = P_P V_e = h\nu_c \alpha \upsilon / c \quad \text{[J] – for a moving electron} \qquad (11)$$

The parameter E_{IFM} with dimensions of energy is called **Inertial Force Moment.** It permits estimation of the deviation energy of folded CL nodes, displaced from its structure at velocity υ**.** The same parameter can be scaled for moving proton (neutron) using the volume ratio between FOHSs of electron and proton (equal to their mass ratio).

$E_{IFM} = (m_p c\alpha)\upsilon$ **- for a moving proton** $E_{IFM} = (m_n c\alpha)\upsilon$ **- for a moving neutron** (12)

The inertial force moment for atom with atomic mass A is:

$E_{IFM} = (c\alpha Au)\upsilon$ where: A – atomic mass, u – atomic mass unit (13)

Note: E_{IFM} **should not be confused with the kinetic energy.**

Eq. (13) permits to transfer the concept of folded node energy to a massive solid object. The analysis of the force moment of a real body with mass m in the initial moment of a free fall under acceleration g leads to the expression: $\Delta E_{IFM} = \alpha cmg$ Its gravitational potential is: $U_G = GMm/R$ .Dividing ΔE_{IFM} on U_G we get the useful expression:

$$U_G / \Delta E_{IFM} = R/(\alpha c) \quad \text{[s]} \qquad (14)$$

Let estimate Eq. (14) for a Compton time unit when its left side is equal to one. **We obtain**:

$$R = \alpha c / \nu_c = 1.7706 \times 10^{-14} (m) \qquad (15)$$

This is twice the small radius of electron (see Fig. 7): $2r_e = 1.7685 \times 10^{-14} (m)$

Conclusion: CL nodes folds and deviate around the small electron radius (which is the same for all negative FOHSs) – **inertial interaction**

Fig. 18 shows a plot of Eq. (14) using planet and moon data from NASA fact data sheets. All points lie on the predicted theoretical line.

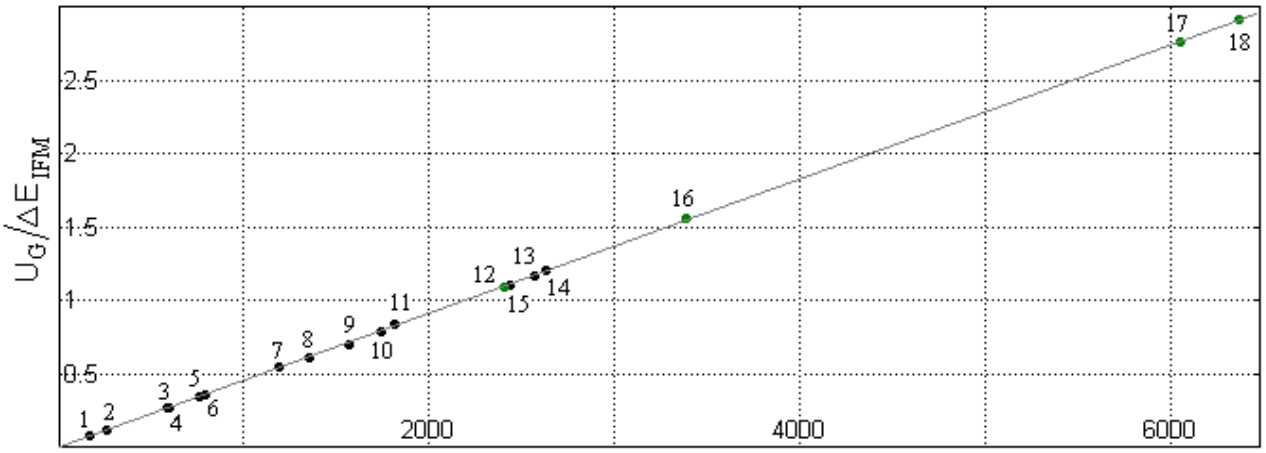

Fig. 18.

Planets and moons in increasing order of their radius are shown as numbers. Number 15 (Mercury), however, appears in a reversed position. This anomaly is studied by plotting the mass of the planets and moons toward their volume as shown in Fig.19. It leads to formulation of hypothesis that protons and neutrons may crush under enormous gravitational pressure forming a denser bunch of straight FOHSs. Such formation may cause a **strong magnetic field**. The analysis of the solar planets and moons and also the pulsar formations from collapsing stars and their features agree with this hypothesis (BSM, Chapters 10&12).

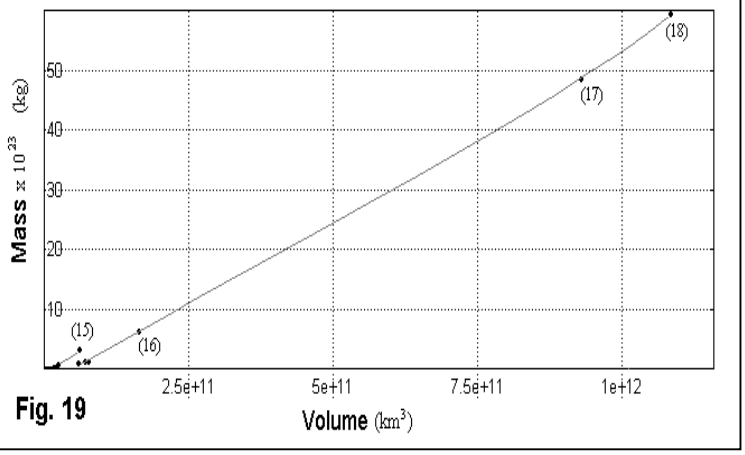

Fig. 19

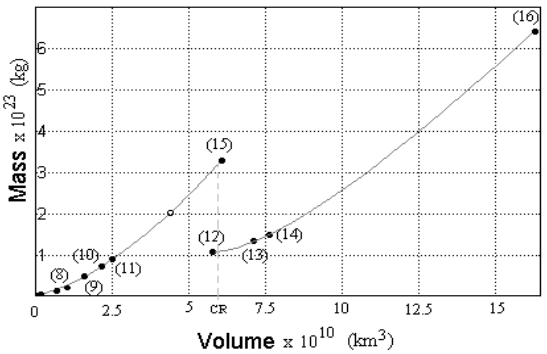

Expanded view of the broken trend

The tangential velocity of a planet with mass M_M in a circular orbit around a star with mass M_S is $\upsilon = (GM_S / r)^{1/2}$. The square of the ratio between the inertial force moment and kinetic energy of the planet is

$$\left[\frac{E_{IFM}}{E_K}\right]^2 = \frac{4\alpha^2 c^2}{GM_S} r = C_E r \qquad (16)$$

Using the solar mass $M_S = 1.9891 \times 10^{30} (kg)$, the predicted value for CE is: $C_E = 1.44238 \times 10^{-7}$. Plotting the left side of Eq. (16) towards mean orbital radius r (using planets and moons data), one obtains a well-defined linear plot. The slop of this line gives a value of C_E, witch differs from the predicted one only by 0.06%.

Conclusions:

All expressions from (11) to (16) and corresponding plots indicate that the **fine structure constant (α) plays an important role in the inertial interactions**.

The ratio between the Partial and Static CL pressure is a function only of the fine structure constant:

$$P_P \big/ P_S = \alpha^2 \big/ \sqrt{1-\alpha^2} \qquad (17)$$

For any objects or system P_P is related to its mass and P_S to its dynamics. Then Eq. (17) indicates that CL space defines a preferable ratio between the mass of a system and its kinetic energy.

In Chapter 12 a theoretical model of the fine structure constant as a ratio between two rotational periods of IG modes (similar to SPM and NRM periods for CL node) in the primary tetrahedron of FPs is presented. It leads to the expression:

$$\alpha_c = 2\big/[(n^2+2\pi^2)^{1/2}+n] = 7.29735194\times10^{-3} \quad \text{for n = 137} \qquad (18)$$

$$\alpha = 7.2973525\times10^{-3} \quad \text{(CODATA 98)}$$

Interpretation of the Einstein's equation $E = mc^2$: According to BSM, mass is not equivalent to matter, so the interpretation of this equation as annihilation or creation of matter is incorrect. While the equation is always true, the correct interpretation is:

$mc^2 \rightarrow E$ - destruction of mass (in particle collider experiments) or hiding of the positron's mass (in the above example of positronium)

$E \rightarrow mc^2$ - creation of a virtual particle, not possessing matter)

$E \Leftrightarrow mc^2$ - valid for the binding energy in atomic nuclei, as a result of small change of the CL space internode distance in presence of matter.

BSM concept leads to a new vision about the space, microcosmos and Universe: The analysis of experiments and observations provided in BSM Chapter 12 leads to the conclusion that the galactic red shift is not of Doppler type, but from inhomogeniety of the different galactic spaces, so the Universe is stationary. Many enigmatic cosmological phenomena get reasonable explanations. Every galaxy has own "Big Bang" cycle with a detectable signature – GRB.

Major conclusions:

- **The speed of light** appears independent from velocity since the Doppler shift and clock rate change cancel each other (effect described by Ronald R. Hatch). The Michelson-Morley experiment is inconclusive due to this effect. Laboratory and field experiments for detection of Earth and solar system motion through space exist.
- **The space in which we live and observe** contains underlying superfine material structure, which define the Quantum Mechanical and Relativistic properties of the physical vacuum.
- **The space contains hidden energy, which is not of EM type.**
- **Gravitation and inertia are not intrinsic features. They could be manageable – a promising opportunity for distant space flights.**

Author's publications, related to Basic Structures of Matter hypothesis:

I. In peer reviewed journals

[1]. S. Sarg, A Physical Model of the Electron according to the Basic Structures of Matter Hypothesis, Physics Essays, International Journal Dedicated to Fundamental Questions in Physics, vol. 16 No. 2, 180-195, (2003); http://www.physicsessays.com

[2]. S. Sarg, Brief introduction to Basic Structures of Matter theory and derived atomic models, Journal of Theoretics (Extensive papers), January, 2003; http://www.journaloftheoretics.com

[3]. S. Sarg, Atlas of Atomic Nuclear Structures according to the Basic Structures of Matter Theory, Journal of Theoretics (Extensive papers, March, 2003); http://www.journaloftheoretics.com

[4]. S Sarg, Application of BSM atomic models for theoretical analysis of biomolecules (with three formulated hypotheses), Journal of Theoretics, May 2003; http://www.journaloftheoretics.com

II. In electronic archives

[5] S. Sarg ©2001, *Basic Structures of Matter*, monograph thesis. http://www.helical-structures.org
also in: http://www.nlc-bnc.ca/amicus/index-e.html (First edition, 2002; Second edition, 2005), (AMICUS No. 27105955), Canadiana: 20020076533; LC Class no.: QC794.6*; Dewey: 530.14/2 21

[6] S. Sarg © 2001, *Atlas of Atomic Nuclear Structures*, monograph http://www.helical-structures.org
also in: http://www.nlc-bnc.ca/amicus/index-e.html (April, 2002), (AMICUS No. 27106037); Canadiana: 2002007655X; ISBN: 0973051515, LC Class: QC794.6*; Dewey: 530.14/2 21

[7] S. Sarg, *New vision about a controllable fusion reaction*, monograph. http://www.nlc-bnc.ca/amicus/index-e.html (April, 2002); (AMICUS No. 27276360); Canadiana: 20020075960;

[8] S. Sarg, New approach for building of unified theory,
http://lanl.arxiv.org/abs/physics/0205052 (May 2002)

III. International conferences

[9] S. Sarg, How an alternative concept of the physical vacuum leads to a different vision about the Universe, "Universe, Nature and Humankind", 28 – 30 Nov 2003, Sofia, Bulgaria

[10] S. Sarg, Basic Structure of Matter Hypothesis Based on an Alternative Concept of the Physical Vacuum (poster report), "Physics for the Third Millenium" Conference, organized by NASA, Huntsville Al, USA, 5-7 Apr 2005.

IV. Books

[10] S. Sarg, *Beyond the Visible Universe*, Helical Structures Press, 2004

Acknowledgements:

International sponsorship including The Planetary Association for Clean Energy, Inc. Ottawa, http://pacenet.homestead.com